New collective structures in ^{179}Au and their implications for the triaxial deformation of the ^{178}Pt core

M. Balogh,[1,2] E. Jajčišinová,[1] M. Venhart,[1,*] A. Herzáň,[1] J. L. Wood,[3] D. T. Joss,[4] F. A. Ali,[4,5] K. Auranen,[6] S. Bánovská,[1] M. Bírová,[1] R. J. Carroll,[4] D. M. Cox,[7] J. G. Cubiss,[8] T. Davis,[4] M. C. Drummond,[4] P. T. Greenlees,[6] T. Grahn,[6] A. Gredley,[4] J. Henderson,[9] U. Jakobsson,[6] R. Julin,[6] S. Juutinen,[6] G. Kantay,[1] J. Konki,[6] P. Konopka,[1] M. Leino,[6] V. Matoušek,[1] A. K. Mistry,[10] C. G. McPeake,[4] D. O'Donnell,[11] R. D. Page,[4] J. Pakarinen,[6] P. Papadakis,[6,†] J. Partanen,[6,‡] P. Peura,[6] P. Rahkila,[6] P. Ruotsalainen,[6] M. Sandzelius,[6] J. Sarén,[6] B. Saygı,[12] M. Sedlák,[1,2] D. Seweryniak,[13] C. Scholey,[6] J. Sorri,[6,§] A. Špaček,[1] S. Stolze,[6,‖] M. Taylor,[14] A. Thornthwaite,[4] J. Uusitalo,[6] M. Veselský,[15] S. Vielhauer,[1] and F. P. Wearing[4]

[1]*Institute of Physics, Slovak Academy of Sciences, SK-84511 Bratislava, Slovakia*
[2]*INFN Laboratori Nazionali di Legnaro, IT-35020 Padova, Italy*
[3]*Department of Physics, Georgia Institute of Technology, Atlanta, Georgia 30332, USA*
[4]*Department of Physics, Oliver Lodge Laboratory, University of Liverpool, Liverpool L69 7ZE, United Kingdom*
[5]*Department of Physics, College of Science Education, University of Sulaimani, P.O. Box 334, Sulaimani, Kurdistan Region, Iraq*
[6]*Accelerator Laboratory, Department of Physics, University of Jyväskylä, FI-40014 Jyväskylä, Finland*
[7]*Department of Physics, Lund University, 22100 Lund, Sweden*
[8]*Department of Physics, University of York, York YO10 5DD, United Kingdom*
[9]*Department of Physics, University of York, Heslington, York YO10 5DD, United Kingdom*
[10]*Institut für Kernphysik, Technische Universität Darmstadt, Darmstadt D-64289, Germany*
[11]*School of Computing, Engineering & Physical Sciences, University of the West of Scotland, Paisley PA1 2BE, United Kingdom*
[12]*Ege University, Faculty of Science, Department of Physics, 35100 Bornova, Izmir, Turkey*
[13]*Physics Division, Argonne National Laboratory, Argonne, Illinois 60439, USA*
[14]*The University of Manchester, School of Physics and Astronomy, Oxford Road, M13 9PL Manchester, United Kingdom*
[15]*Institute of Experimental and Applied Physics, Czech Technical University, Prague 110 00, Czech Republic*

(Received 9 May 2022; accepted 21 November 2022; published 22 December 2022)

The extremely neutron-deficient isotope ^{179}Au has been studied by a combination of in-beam γ-ray and isomeric-decay spectroscopy. For in-beam spectroscopy, the recoil-isomer tagging technique was employed, using the known $3/2^-$, $T_{1/2} = 328$ ns isomer. A new rotational band, associated with the unfavored signature band of the $1h_{9/2} \oplus 2f_{7/2}$ proton-intruder configuration, was revealed. A previously unknown, high-spin isomeric state with an excitation energy of 1743(17) keV and $T_{1/2} = 2.16(8)$ µs was discovered. Five decay paths were identified, some of them feeding previously unknown non-yrast excited states, associated with the $1i_{13/2}$ proton-intruder configuration. Calculations based on the particle-plus-triaxial-rotor model were performed to interpret the data. On the basis of these calculations, the new $1h_{9/2} \oplus 2f_{7/2}$ rotational band is interpreted as due to triaxial deformation of the underlying configuration with $\beta_2 \approx 0.26$ and $\gamma \approx 27^\circ$. Observed non-yrast states of the positive-parity $1i_{13/2}$ intruder configuration are interpreted as due to triaxial deformation with $\beta_2 \approx 0.26$ and $\gamma \approx 20^\circ$.

DOI: 10.1103/PhysRevC.106.064324

I. INTRODUCTION

The odd-mass Au isotopes offer a broad systematic view of nuclear structure in a region of near-degenerate, multiple coexisting shapes [1]. The most neutron-deficient Au isotopes have been the subject of an extensive program of investigation using γ-ray and conversion-electron studies following β decay [2–8], in-beam reaction γ-ray spectroscopy [9–24], spectroscopy of directly produced isomeric states [25,26], in-beam isomer-tagged studies [27], laser-induced hyperfine spectroscopy [28–30], and α-decay studies of odd-mass Tl isotopes [25,31–33]. Nevertheless, in comparison to the heavier Tl and Au isotopes, where multiple shape coexistence has been established [1,4,34,35], a rich variety of structures remain to be discovered. Indeed, already it is evident that there are new structures in ^{177}Au [20] and ^{179}Au [25] that have no counterpart in the heavier Au isotopes, as far as current spectroscopy has revealed. Thus, much work still needs to be done if a thorough understanding of shape coexistence is to be achieved in this region, and by implication in all mass

*Corresponding author: martin.venhart@savba.sk
†Present address: STFC Daresbury Laboratory, Daresbury, Warrington WA4 4AD, United Kingdom.
‡Deceased.
§Present address: STUK - Radiation and Nuclear Safety Authority, P.O. BOX 14, 00811 Helsinki, Finland.
‖Present address: Physics Division, Argonne National Laboratory, Argonne, Illinois 60439, USA.

regions. We note a very recent claim of longitudinal wobbling (a potential feature of a triaxial rotor) in ^{187}Au [36], and its refutation [37].

In the details, there are many unanswered questions, especially in the case of lighter Au isotopes. First, how many different deformed structures are there? In ^{187}Au the conclusion is four different shapes [4]. Second, what role does triaxial deformation play? Again, in ^{187}Au the conclusion is that it is critical [4]. However, establishing triaxial deformation in a reliable manner necessitates the identification of non-yrast structures. Such structures are not observed in typical survey-type studies because they require long running times on accelerators due to their weak population; and at the extremes of stability this extends to beam time measured in weeks. In the present study, we used in-beam γ-ray spectroscopy with a selective isomer-tagging technique in combination with isomer decay spectroscopy to address the above questions in ^{179}Au.

A spin-parity of $1/2^+$ has been unambiguously established for the ^{179}Au ground state by the in-source laser spectroscopy experiment [28], performed with the RILIS ion source at the CERN-ISOLDE facility. The first information on excited states in ^{179}Au came from an in-beam γ-ray spectroscopy experiment, performed at the Gammasphere array [15]. It revealed four rotational bands, associated with the $1h_{9/2} \oplus 2f_{7/2}$ and $1i_{13/2}$ proton-intruder configurations. The observed $9/2^-$ bandhead excitation energy was not established; note the Δ and x symbols in the level scheme shown in Fig. 2 of [15]. An excitation energy of 134(15) keV was established for the $9/2^-$ state by an α-decay study of ^{183}Tl^m [25]. It involved combined data acquired at the RITU separator at Jyväskylä and at the ISOLDE facility.

In this study, an isomeric state with a spin-parity of $3/2^-$ and $T_{1/2} = 328$ ns was discovered. This isomer played a major role in advancing the understanding of nuclear structure of odd-mass Au isotopes. Its discovery initiated a focused research program, which resulted in a significant extension of the systematics of the excited states of odd-mass Au isotopes beyond the $N = 104$ midshell point [2,3,20,27]. The isomer has two parallel decay branches, feeding the $1/2^+$ ground state: the 62.4–27.1 keV cascade and the 89.5 keV crossover transition. Both the 62.4 and 89.5 keV transitions were unambiguously shown to have a retarded $E1$ nature [25] and therefore they are only weakly converted. Another in-beam study [27] suggested modifications to the level scheme proposed in [15]. Very recently a comprehensive study of decay modes of ^{183}Tl^m was performed at ISOLDE, which extended the decay scheme given in [25]. A slightly lower excitation energy of 127(17) keV was determined for the $9/2^-$ state in ^{179}Au. The 127 keV $9/2^-$ state and the 89.5 keV $3/2^-$ state are assumed to be connected by transition(s) which are not observed; see [25] for details.

This article reports on a study of the ^{179}Au isotope, located 18 neutrons away from the stable ^{197}Au. A new rotational band was revealed by means of in-beam γ-ray spectroscopy with application of the recoil-isomer tagging technique. Furthermore, a new, high-spin isomeric state was discovered. Deexcitation paths of the isomer revealed hitherto unknown excited states. These states, together with the new rotational band, indicate strong triaxial deformation for the intruder configurations in ^{179}Au. This interpretation is based on calculations with the particle-plus-triaxial-rotor model (PTRM) [38].

II. EXPERIMENTAL DETAILS

The experiment was performed at the Accelerator Laboratory of the University of Jyväskylä. The ^{179}Au nuclei were produced using the ^{100}Ru(^{82}Kr, $p2n$)^{179}Au reaction. A beam of ^{82}Kr^{15+} ions with kinetic energy of 352 MeV was delivered by the $K = 130$ MeV cyclotron and impinged on a self-supporting metallic target produced from isotopically enriched ^{100}Ru metal. For detection of prompt γ rays, the target chamber was surrounded by the JUROGAM-II array, composed of 10 Eurogam Phase I type coaxial and 24 Euroball clover germanium detectors arranged into three rings relative to the beam direction, and equipped with active BGO Compton-suppression shields.

The RITU gas-filled separator [39] was used for in-flight separation of reaction products from the primary beam according to their different magnetic rigidities. The detection system GREAT [40] was employed at the focal plane of the separator. At the entrance of the GREAT spectrometer, recoiling nuclei passed through a multiwire proportional counter. It provided discrimination of evaporation residues from radioactive decays. Subsequently, nuclei were implanted into a double-sided silicon strip detector (DSSD). For detection of γ rays at the focal plane, a planar double-sided HPGe strip detector and an array of three HPGe clover detectors were employed. The planar detector was placed inside the vacuum chamber, separated from the DSSDs by a thin beryllium window. Signals from all detectors were processed by a fully digital data acquisition system, based on commercial Lyrtech digitizers, and stored on disk as a time-stamped data stream. This data format allowed an offline analysis to be performed by construction of various coincidences. The data obtained from the 267 hour long experiment were sorted using the dedicated GRAIN software [41].

III. EXPERIMENTAL RESULTS

A. In-beam spectroscopy of the negative-parity intruder configuration

The long half-life of the $1/2^+$ ground state ($T_{1/2} = 7.1(3)$ s [42]) in combination with a high recoil-implantation rate (on average 3.5 recoils per 20 s) prevented an effective use of the recoil-decay tagging method [43]. Instead, the recoil-isomer tagging [44,45] technique was employed to identify prompt γ rays feeding the $9/2^-$ intruder state in ^{179}Au. The isomeric 62.4 and 89.5 keV γ rays were used as a tag for a $\gamma - \gamma$ coincidence matrix. In addition, a recoil-gated triple-γ coincidence cube was constructed. Note that due to limited statistics, an isomer-tagged cube could not be created. On the basis of coincidence relationships of the observed γ rays, the level scheme shown in Fig. 1 is proposed. Note that the same numbering of rotational bands as in the previous in-beam study [15] of ^{179}Au is used. Prompt γ rays observed

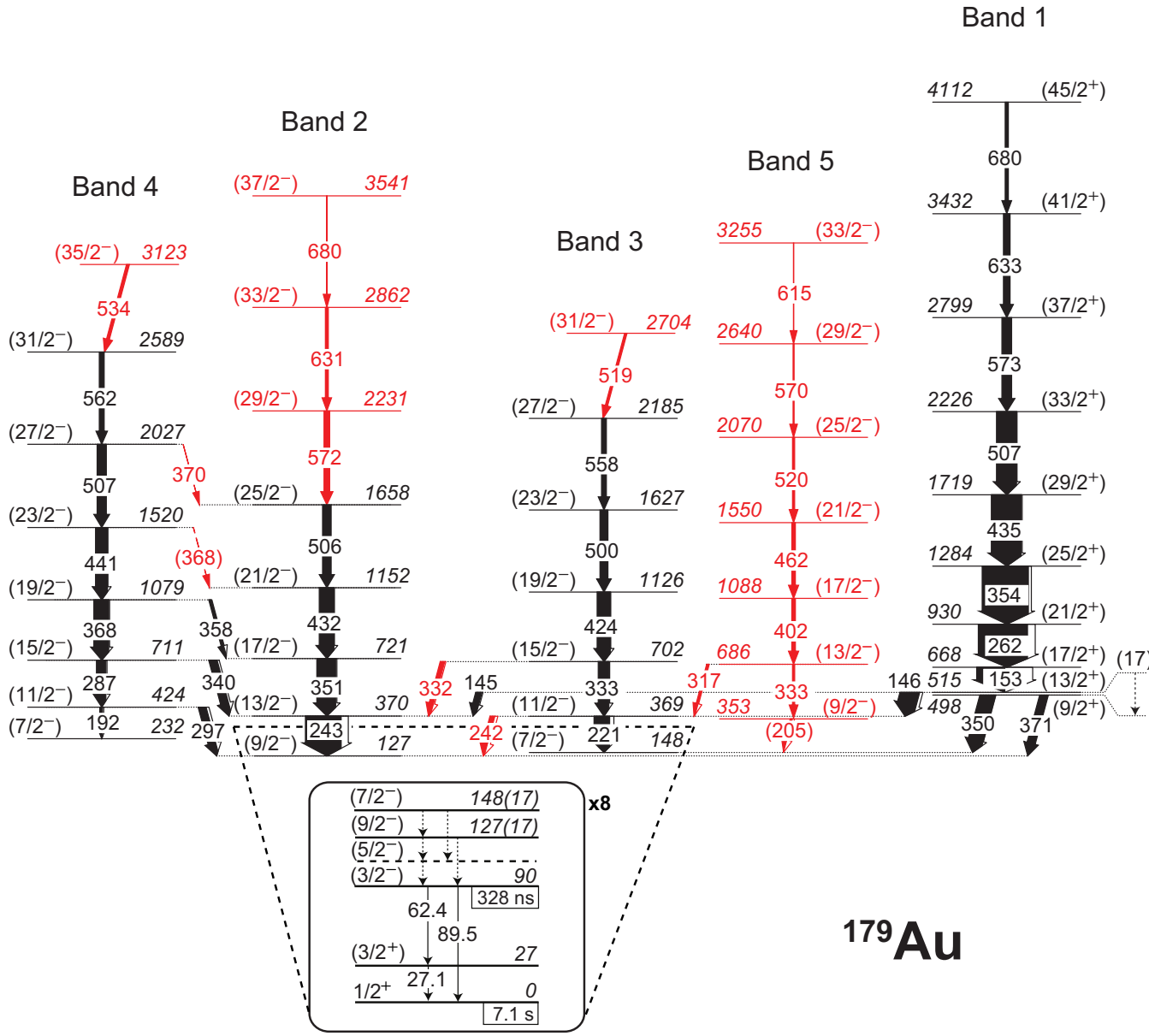

FIG. 1. Partial level scheme of ^{179}Au combining the previous studies [15,25,27] and results of the present work, indicated with red color. Four energy levels in Band 1 with spin greater than $45/2^+$ are not shown [15]. The widths of the arrows are proportional to the transition intensities extracted from this work. The black box contains an 8× magnified low-energy part of ^{179}Au level scheme. Note that the $9/2^-$ state decays via unknown, low-energy transitions marked with dotted arrows to the $3/2^-$ isomeric state; see [25] for details.

in the present experiment unambiguously assigned to ^{179}Au are listed in Table I.

Figure 2(a) shows a summed spectrum of γ rays detected in coincidence with the 401.9 and 461.6 keV γ rays. A cascade of the 316.9, 401.9, 461.6, and 520.2 keV γ-ray transitions is observed. These γ-ray transitions form a new rotational band denoted as Band 5 in the level scheme. Figure 2(b) gives a spectrum of coincident γ rays, gated on the 520.2 keV γ ray. In addition to the aforementioned cascade, the 570.3 and 615 keV γ rays are observed, which extend the new band. The 520.2 keV transition from Band 5 is a doublet with a newly identified 519.1 keV transition from Band 3; see the discussion below. Therefore, the 333.2, 424.0, and 558.3 keV γ rays contaminate the spectrum.

The 316.9 keV transition is the only interband transition observed to link Band 5 with the rest of the level scheme. It depopulates the $13/2^-$ state, feeding the known $11/2^-$ member of Band 3. Additional supporting arguments for this assignment are given later in the text.

Figure 3(a) gives a projection of the triple-γ cube with a double gate on the 243.0 and 431.9 keV γ rays, which are known transitions in Band 2. Two previously unknown 572.4 and 631.0 keV γ rays are observed. Figure 3(b), gives a spectrum of coincident γ rays with a double gate on the 431.9

TABLE I. Band assignments, transition energies (E_γ), relative γ-ray intensities (I_γ) from the JUROGAM-II data, energies of the initial and final states (E_i and E_f), initial and final spin-parities (J_i^π and J_f^π), respectively, for the γ-ray transitions assigned to ^{179}Au. Experimental uncertainties of the γ-ray energies are ± 0.5 keV. If a value is given without a decimal point, the γ-ray energy uncertainty is ± 1 keV. The γ-ray intensities were extracted using the absolute coincidence intensity method [47].

Band	E_γ (keV)	I_γ (%)	E_i (keV)	J_i^π	E_f (keV)	J_f^π
1	153.2	57(5)	668	$(17/2^+)$	515	$(13/2^+)$
1	262.3	100(5)	930	$(21/2^+)$	668	$(17/2^+)$
1	354.2	94(6)	1284	$(25/2^+)$	930	$(21/2^+)$
1	434.7	60(4)	1719	$(29/2^+)$	1284	$(25/2^+)$
1	507.1	41(3)	2226	$(33/2^+)$	1719	$(29/2^+)$
1	573.4	19.4(19)	2799	$(37/2^+)$	2226	$(33/2^+)$
1	633.1	13.2(18)	3432	$(41/2^+)$	2799	$(37/2^+)$
1	680.3	6.4(10)	4112	$(45/2^+)$	3432	$(41/2^+)$
$1 \rightarrow 2$	145.3	12(3)	515	$(13/2^+)$	369	$(13/2^-)$
$1 \rightarrow 2$	371.0	16.9(20)	498	$(9/2^+)$	127	$(9/2^-)$
$1 \rightarrow 3$	145.7	39(8)	515	$(13/2^+)$	369	$(11/2^-)$
$1 \rightarrow 3$	350.0	31.0(25)	498	$(9/2^+)$	148	$(7/2^-)$
2	243.0	73(7)	370	$(13/2^-)$	127	$(9/2^-)$
2	350.6	38(3)	721	$(17/2^-)$	370	$(13/2^-)$
2	431.9	24.2(18)	1152	$(21/2^-)$	721	$(17/2^-)$
2	505.7	13.1(14)	1658	$(25/2^-)$	1152	$(21/2^-)$
2	572.4	7.6(10)	2231	$(29/2^-)$	1658	$(25/2^-)$
2	631.0	3.0(7)	2862	$(33/2^-)$	2231	$(29/2^-)$
2	680.0	1.1(5)	3541	$(37/2^-)$	2862	$(33/2^-)$
3	221.0	32(5)	369	$(11/2^-)$	148	$(7/2^-)$
3	333.2	22(5)	702	$(15/2^-)$	369	$(11/2^-)$
3	424.0	27(4)	1126	$(19/2^-)$	702	$(15/2^-)$
3	500.5	15.8(15)	1627	$(23/2^-)$	1126	$(19/2^-)$
3	558.3	9.7(11)	2185	$(27/2^-)$	1627	$(23/2^-)$
3	519.1	4.6(14)	2704	$(31/2^-)$	2185	$(27/2^-)$
$3 \rightarrow 2$	242.4	10(4)	369	$(11/2^-)$	127	$(9/2^-)$
$3 \rightarrow 2$	332.2	9(4)	702	$(15/2^-)$	370	$(13/2^-)$
4	192.3	5.6(8)	424	$(11/2^-)$	232	$(7/2^-)$
4	286.5	24.8(13)	711	$(15/2^-)$	424	$(11/2^-)$
4	368.0	28.3(22)	1079	$(19/2^-)$	711	$(15/2^-)$
4	441.0	27.1(21)	1520	$(23/2^-)$	1079	$(19/2^-)$
4	507.2	19(3)	2027	$(27/2^-)$	1520	$(23/2^-)$
4	562.5	9.7(25)	2589	$(31/2^-)$	2027	$(27/2^-)$
4	533.7	5.7(14)	3123	$(35/2^-)$	2589	$(31/2^-)$
$4 \rightarrow 2$	297.4	14.7(16)	424	$(11/2^-)$	127	$(9/2^-)$
$4 \rightarrow 2$	340.4	15.5(15)	711	$(15/2^-)$	370	$(13/2^-)$
$4 \rightarrow 2$	358.2	5.1(11)	1079	$(19/2^-)$	721	$(17/2^-)$
$4 \rightarrow 2$	(368)	<2	1520	$(23/2^-)$	1152	$(21/2^-)$
$4 \rightarrow 2$	370	<2	2027	$(27/2^-)$	1658	$(25/2^-)$
5	333.1	4.1(9)	686	$(13/2^-)$	353	$(9/2^-)$
5	401.9	7.0(15)	1088	$(17/2^-)$	686	$(13/2^-)$
5	461.6	7.0(14)	1550	$(21/2^-)$	1088	$(17/2^-)$
5	520.2	4.2(8)	2070	$(25/2^-)$	1550	$(21/2^-)$
5	570.3	2.0(7)	2640	$(29/2^-)$	2070	$(25/2^-)$
5	615	0.6(6)	3255	$(33/2^-)$	2640	$(29/2^-)$
$5 \rightarrow 3$	(205)		353	$(9/2^-)$	148	$(7/2^-)$
$5 \rightarrow 3$	316.9	3.9(6)	686	$(13/2^-)$	369	$(11/2^-)$

and 631.0 keV γ rays. A new γ ray at 680.0 keV is seen. The 572.4, 631.0, and 680.0 keV transitions are assigned as an extension of Band 2.

Figure 4 gives a projection of the triple-γ cube with a double gate on the 243.0 and 562.5 keV γ rays. The new 368 and 370 keV γ rays are observed. They are interpreted as linking transitions connecting Band 4 with Band 2. Note that in the spectrum the 368 keV γ ray overlaps with the energy of the $19/2^- \rightarrow 15/2^-$ transition in Band 4, therefore only a tentative assignment could be made for this transition.

Figure 5 gives a spectrum of γ rays detected in coincidence with the 333 keV multiplet (overlapping transitions in Band 3

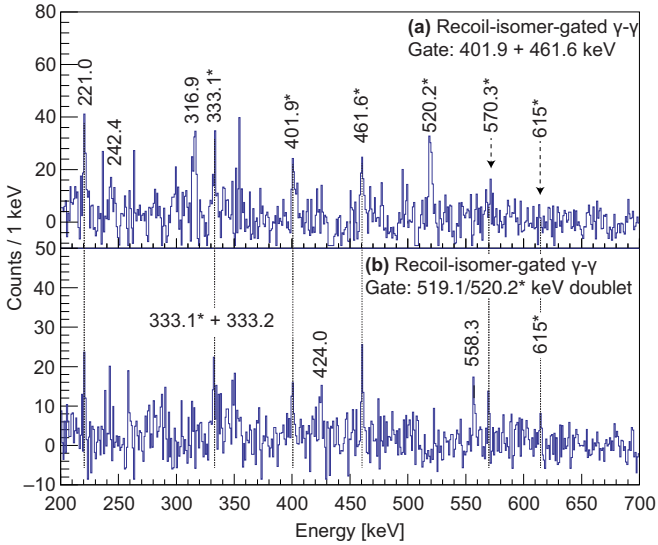

FIG. 2. Background-subtracted coincident γ-ray energy spectra with (a) a sum gate on the 401.9 and 461.6 keV transitions, and (b) a gate on the 519.1/520.2 keV doublet in the coincidence matrix tagged with the 328 ns isomeric state. The asterisk symbols mark in-band transitions belonging to Band 5.

and Band 5). A coincidence between the 243 and 333 keV γ rays was attributed to a ^{179}Hg contamination in the previous in-beam study [15]. However, the known 121.1, 392.0, 417.1, 476.0, and 492.6 keV γ rays of ^{179}Hg [46] are not observed here. Therefore, the observed coincidence between the 243.0 and 333.2 keV γ rays is assigned to ^{179}Au. An explanation of this pattern is that the 242.4 and 332.2 keV transitions connect Band 3 with Band 2; see the level scheme given in Fig. 1. Due to insufficient energy resolution, only the

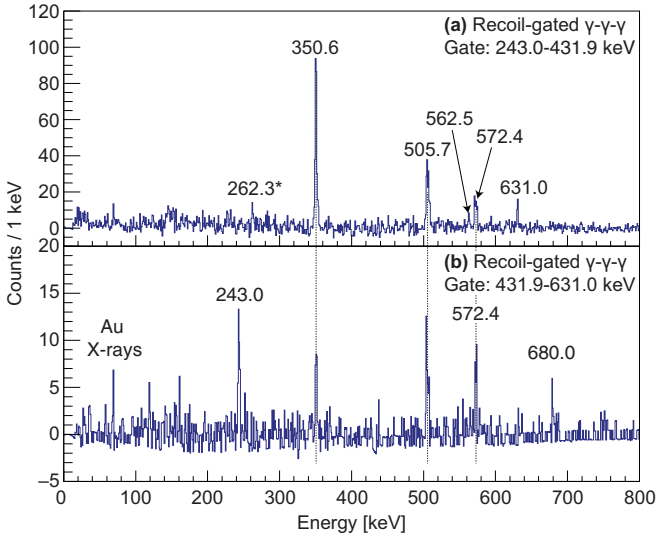

FIG. 3. Background-subtracted double-gated recoil-tagged coincident γ-ray energy spectra. Double gates are set on the (a) 243.0–431.9 keV, and (b) 431.9–631.0 keV transitions. The 262.3 keV peak marked with an asterisk in spectrum (a) is due to contamination from Band 1.

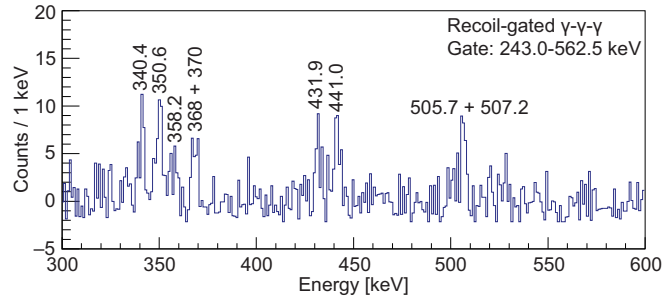

FIG. 4. Background-subtracted recoil-tagged γ-ray energy spectrum with double gate set on the 243.0 and 562.5 keV transitions.

γ-ray doublets with the in-band transitions are observed in our spectra: the $(15/2^-)$ state in Band 3 is depopulated by the 333.2/332.2 keV doublet; and the $9/2^-$ state in Band 2 is populated through the 242.4/243.0 keV doublet. Energies of the new 242.4 and 332.2 keV transitions were deduced from the energy differences between the respective levels. The results of the absolute coincidence intensity analysis [47] shown in Table I unambiguously show the presence of both γ-ray interband transitions.

Note that the 316.9 keV γ ray is not observed in the spectrum given in Fig. 5, which corroborates the proposed level scheme. A weak 205 keV γ-ray peak is tentatively interpreted as the deexcitation of the Band 5 bandhead, feeding the $7/2^-$ state of Band 3.

In the 520 keV gated spectrum [see Fig. 2(b)], transitions other than those belonging to Band 5 are observed, namely the 424.0 and 558.3 keV transitions of Band 3. Analysis using the "running gate" technique [4] revealed that the 520 keV peak is a 519.1/520.2 keV doublet. Based on the coincidence relationship, the 519.1 keV transition is placed as the topmost transition of Band 3. Furthermore, a new 533.7 keV transition was identified to feed the $31/2^-$ state of Band 4; see Fig. 1.

B. Decay of high-spin isomer

Figure 6(a) gives a spectrum of γ-ray singles, detected with the clover-detector array at the focal plane within a 7 μs time window after recoil implantation. Only events that were followed by a subsequent detection of the 62.4 keV γ ray with the planar detector were accepted, i.e., those that were

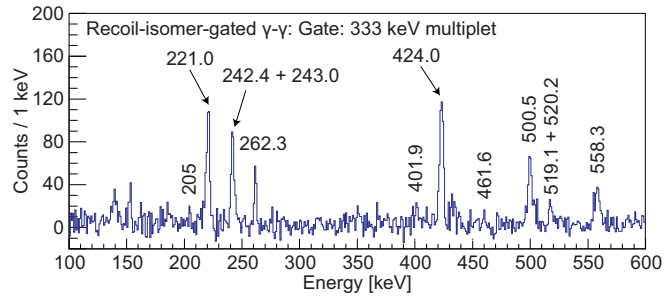

FIG. 5. Background-subtracted coincident γ-ray energy spectrum with gate set on the 333 keV multiplet in the coincidence matrix tagged with the 328 ns isomeric state.

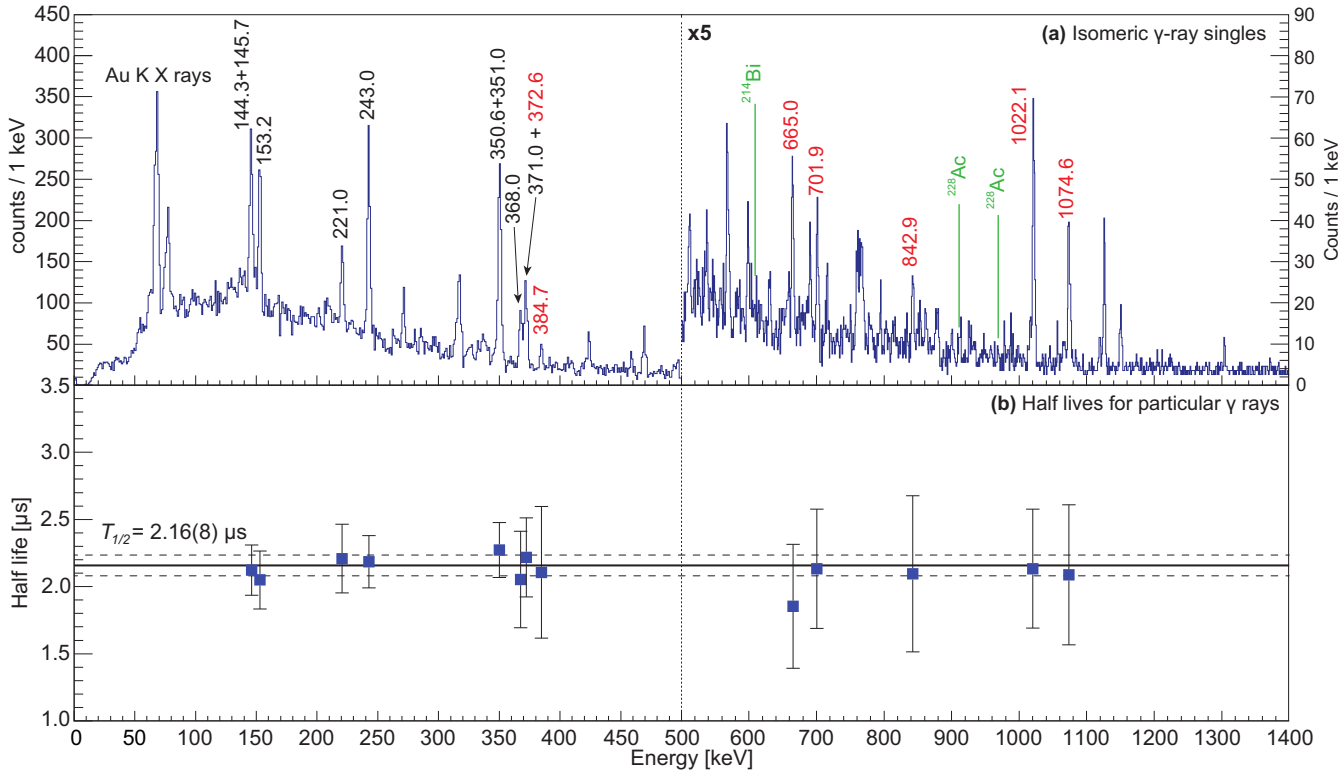

FIG. 6. (a) Spectra of γ-ray singles detected with the focal-plane clover-detector array within a 7 μs window after recoil implantation, that were followed by delayed detection of the 62.4 keV transition, within a 1.5 μs window. Transitions attributed to the decay of the new isomer in ^{179}Au are annotated with their energies. Other γ rays were not assigned. New transitions are indicated with the red color. Other transitions are known from in-beam studies performed in the present work and in [15,27]. Energies of strong γ rays of naturally occurring ^{214}Bi and ^{228}Ac are indicated. (b) Individual half-lives deduced for particular γ rays, assigned to the decay of the new isomer. Half-lives were determined from distributions of time differences between recoil implantations and γ-ray detections. A half-life of 2.16(8) μs was determined as a weighted average and is indicated in (b) as a full horizontal line; dashed lines mark the confidence interval.

tagged with the decay of the $3/2^-$ isomer. A 1.5 μs window between the detection of recoil and 62.4 keV transition was used. The approach used for identification of the new isomer resembles the standard recoil-isomer tagging technique, applied in prompt γ-ray analysis. Here it is used for the focal-plane detector array. Therefore, γ rays observed in Fig. 6(a) occur *only* due to decay of new isomers in ^{179}Au and feed, directly or indirectly, to the known $3/2^-$ isomer, possibly via elusive low-energy transitions from the $9/2^-$ state. Note that the conventional background subtraction, i.e., comparison of spectra detected within "early" and "late" time gates, is not necessary in this case. Delayed coincidence with the decay of the $3/2^-$ isomer is sufficient to reduce the random background. For example, strong γ rays of naturally occurring ^{214}Bi (609.31 keV) or ^{228}Ac (911.2 and 968.97 keV) nuclides are suppressed to a level below the detection limit. Transitions from natural radioactivity were clearly observed in the spectrum detected within a 7 μs time window after recoil implantation, but without the additional condition for detection of the 62.4 keV γ ray. Note that this spectrum is not given here.

Figure 6(b) gives half-lives for individual γ rays, assigned into the level scheme. Individual half-lives were determined from distributions of time differences between recoil implantations and γ-ray detections, using the statistical method proposed in [48]. Within experimental uncertainties the individual half-lives are equivalent. This suggests that all annotated γ rays occur due to the decay of the same isomeric state. The weighted average of individual half-lives gives $T_{1/2} = 2.16(8)$ μs for the new isomer in ^{179}Au.

To elucidate the decay scheme of the new isomer, analyses of prompt γ-γ coincidences were performed. Figure 7 gives coincidence spectra with gates on the 1022.1, 243.0, 1074.6, 153.2, 701.9, and 665.0 keV γ rays. On the basis of observed coincidence relationships, the decay scheme given in Fig. 8 was constructed. Note that the 665.0, 1022.1, and 1074.6 keV γ-ray transitions feed known structures, revealed by the in-beam spectroscopy, discussed above. Namely, the $17/2^+$ state of Band 1, the $17/2^-$ state of Band 2, and the $19/2^-$ state of Band 4 are fed. The 701.9 keV coincidence gate reveals a hitherto unknown 372.7 keV transition. Relative to the $9/2^-$ state, the excitation energy of the new isomer of 1615.9(4) keV was determined as a weighted average of the sums of γ-ray energies in particular decay paths. This gives an overall excitation energy of 1743(17) keV, relative to the $1/2^+$ ground state. The large experimental uncertainty is caused by the uncertainty on the excitation energy of the $9/2^-$ state.

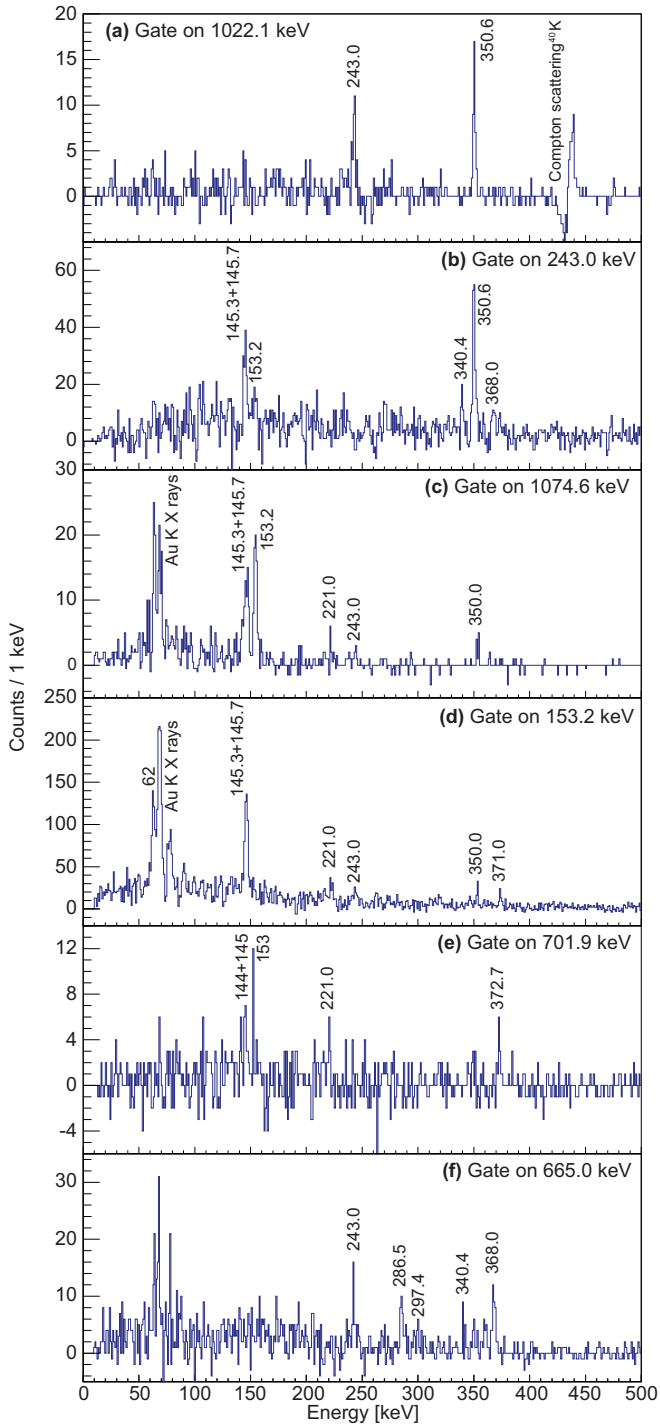

FIG. 7. Coincident γ-ray spectra detected at the focal plane of the separator within a 7 µs window after recoil implantation, with gates on (a) 1022 keV, (b) 243 keV, (c) 1075 keV, (d) 153 keV, (e) 702 keV, and (f) 665 keV transitions.

Relatively weak 842.9 and 384.7 keV peaks are observed in the γ-ray singles spectrum; see Fig. 6. Due to limited statistics, their coincidences could not be investigated. However, the sum of their energies equals that of the 153.2 and 1074.6 keV transitions. Therefore, a 843–385 keV γ-ray cascade is proposed as a competing decay path. Note that no other combination of unassigned γ rays, observed in the singles spectrum, could be placed in the level scheme on the same basis. However, the proposed assignment remains ambiguous. Clear coincidence information, which requires higher statistics, is needed for an unambiguous assignment.

TABLE II. Energies (E_γ), relative γ-ray intensities (I_γ), spin-parity of the final state [J^π(final)], and proposed multipolarity for transitions depopulating the newly discovered isomeric state in ^{179}Au. Note that the 843 keV transition assignment as a transition depopulating the isomer is only tentative; see details given in the text.

E_γ (keV)	I_γ (%)	J_π(final)	Multipolarity
665.0	19(4)	$(19/2^-)$	$(E1)$
701.9	15(4)	$(19/2^+)$	$(M1)$
(842.9)	10(4)	$(15/2^+)$	$(E2)$
1022.1	36(5)	$(17/2^-)$	$(E1)$
1074.6	20(4)	$(17/2^+)$	$(M1)$

Assuming an $M1$ character of both the 701.9 and 1074.6 keV transitions (see discussion below), the ratio of their energy factor of the transition probability is 0.28. In an alternative scenario, where the 701.9 and 372.7 keV transitions were swapped, the same ratio would be only 0.04. In that case the 372.7–701.9 keV cascade would be very weak, compared with the 1074.6 keV transition. This is not observed in the data. The same applies also to the ambiguous 842.9–384.7 keV cascade. Therefore, four deexcitation paths were identified; see the summary given in Table II. Three of them feed known levels and one reveals the existence of a previously unknown excited state. In addition, a tentative path is suggested. Using the number of counts in the spectrum given in Fig. 6, corrected for the respective detection efficiencies, the intensities for particular γ rays were determined. The summary of transitions depopulating the isomer is given in Table II. Possible multipolarities of transitions are discussed below.

We note that multiple γ rays observed in the singles γ-ray spectrum, Fig. 6(a), are left without interpretation due to the lack of γ-γ statistics necessary for unambiguous assignment.

IV. DISCUSSION

To interpret the data, calculations using the particle–triaxial-rotor model [38] with a Woods-Saxon potential for the deformed mean field were performed. The excitation energy of the 2^+ state in the core was estimated using Grodzins' rule. Pairing was treated within the BCS method, therefore the pairing gap Δ and Fermi energy λ were not input parameters. The Hamiltonian was diagonalized within the space of low-lying quasiparticle states. Magnetic dipole matrix elements were calculated using the core $g_R = Z/A$ and an effective spin g_s factor reduced by a factor of 0.7 compared with the free value.

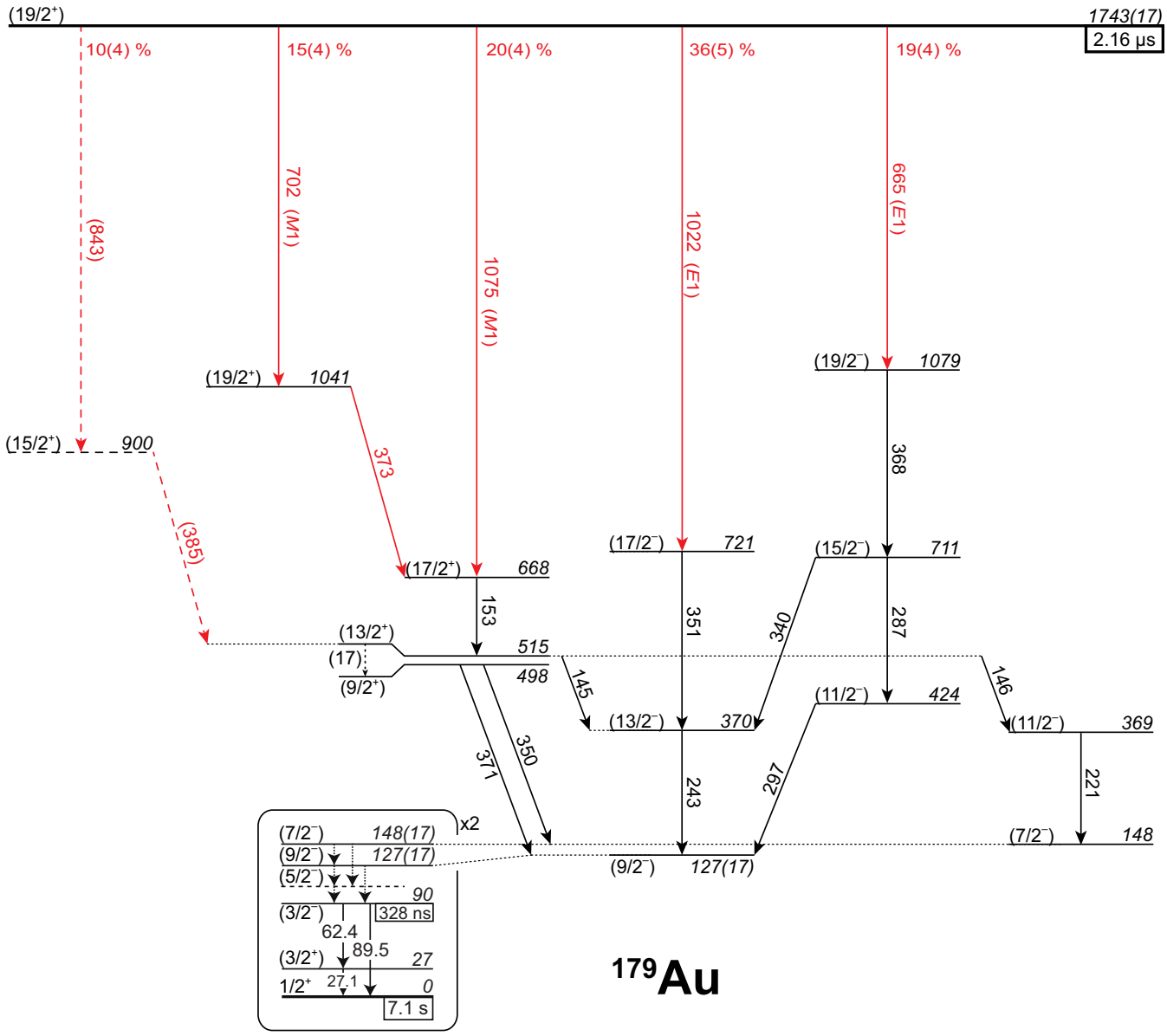

FIG. 8. Decay scheme for the newly discovered isomeric state in ^{179}Au, deduced in the present work. New transitions are highlighted with red color. Note that the $9/2^-$ band head decays through the elusive $5/2^-$ state into the $3/2^-$ isomer [25]. The excitation energy of the $9/2^-$ state was established via α decay of ^{183}Tl [33] with a 17 keV experimental uncertainty. Therefore, the excitation energies of all states given here have this systematic uncertainty. The positive-parity states are associated with the $1i_{13/2}$, negative-parity states with the $1h_{9/2} \oplus 2f_{7/2}$ proton-intruder configurations. The box contains the twice magnified low-energy level scheme of ^{179}Au.

A. Negative-parity intruder states

For negative-parity intruder configurations, the best agreement between calculations and experimental data was reached for $\beta_2 = 0.26$, $\gamma = 27^\circ$, and $\beta_4 = 0.02$; see Fig. 9. Note that the indexing of excited states introduced in Fig. 9 is used later in the text, where other results of the calculations are analyzed.

Figure 10(a) displays the excitation energies of the $5/2^-$, $7/2^-$, $9/2^-_1$, $9/2^-_2$, and $11/2^-_2$ states, relative to the 90 keV $3/2^-$ isomeric state for fixed $\beta_2 = 0.26$ and $\beta_4 = 0.02$ deformation parameters. The triaxial γ parameter was varied within a 0°–30° interval. For all values of γ, the $5/2^-$ state is located slightly above the $3/2^-$ state, which is in agreement with experimental observation. The excitation energy of the $9/2^-_2$ and $11/2^-_2$ states, the bandheads of Band 4 and Band 5, are very sensitive to the triaxial parameter, therefore these bands are of great interest.

Figure 10(b) gives the calculated energy difference between the $9/2^-_2$ and $11/2^-_2$ states for three different values of the β_2 deformation parameters. This is compared with the value determined experimentally in the present work. The best agreement with the data is for γ deformation between 25° and 30°.

Another output of the PTRM calculations is transition intensities. The $13/2^-_2$ state, which is a member of the newly discovered Band 5, deexcites either by an interband transition

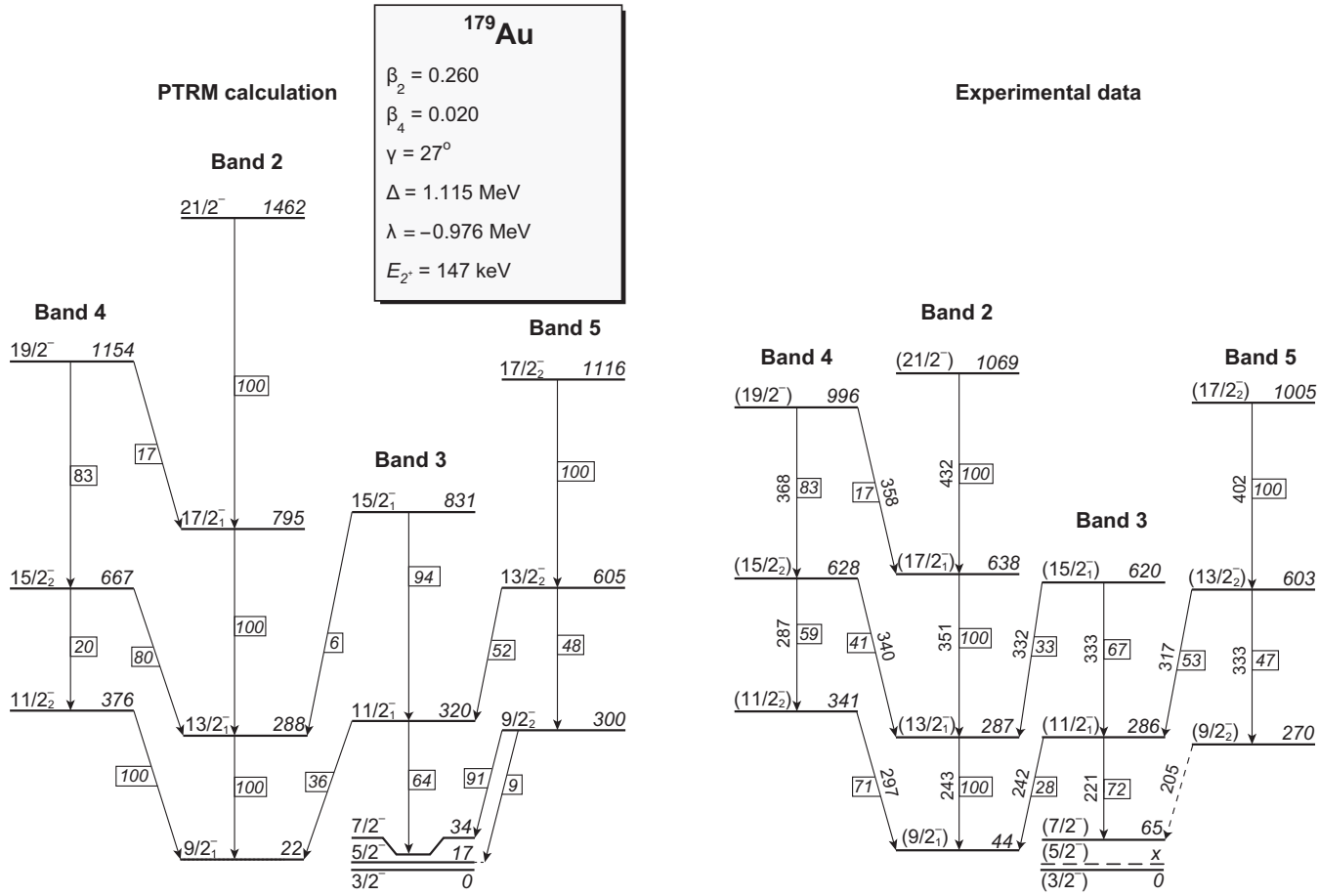

FIG. 9. Comparison of the calculated (left) and experimental (right) decay schemes of states associated with the negative-parity, proton-intruder configurations in ^{179}Au, deduced in the present work. Energies of levels are relative to the 90 keV $3/2^-$ state. Energies of the transitions in the experimental decay scheme are given. Branching rations are given in the boxes. The particle–triaxial-rotor-model, with parameters given in the legend, was used for the calculation.

to the $11/2^-_1$ state of Band 3, or via an in-band transition to the $9/2^-_2$ bandhead. The γ-ray intensity ratio of these transitions was determined to be 1.1(3), i.e., in slight favor of the in-band decay. This ratio has been reproduced with the PTRM code for three different values of the β_2 deformation, and the results are given in Fig. 10(c). The best agreement was reached for a γ deformation at around 27°, which corroborates previous arguments.

Comparison of the PTRM calculations shows in particular the extreme importance of the newly discovered $9/2^-$ band for understanding the triaxial deformation. These bands are very rarely observed due to their non-yrast nature. However, their excitation energies and decay probabilities allow determination of γ.

B. Decay of the isomer and positive-parity intruder states

Excited states associated with the $1i_{13/2}$ and $1h_{9/2}$ proton-intruder configurations are fed from the newly discovered isomer. This indicates that its wave function is dominated by one of these structures. Intruder configurations in odd-mass Au isotopes are known to have proton-particle character, where the odd proton couples with corresponding even-even Pt core [6], resulting in distinct groups of excited states. In ^{178}Pt, which is the core for intruder configurations in ^{179}Au, the 5^- excited state is known at 1573.5 keV [49–51]. Bands based on 5^- excitations are widely observed in even-even isotopes in the studied region of the nuclear chart and their intrinsic structure is still a subject of extensive debates; see [50] and references therein. In the most-recent in-beam study of ^{178}Pt [13], the 5^- state, is interpreted as the decoupled $1h_{9/2}$ two-quasiproton configuration with an admixture of octupole vibrations of unspecified magnitude. Coupling of another $1h_{9/2}$ proton with the 5^- state gives a possible $19/2^+$ assignment for the new isomer in ^{179}Au.

The $19/2^+$ spin-parity assignment is consistent with the observed decay pattern, since the known $17/2^+$, $17/2^-$, and $19/2^-$ states are fed. If the spin of the isomer was higher or lower, feeding of other members of rotational bands would take place. This is not seen in the data. The absence of direct feeding of $15/2^-$ states, that exist in ^{179}Au [15,25] excludes the $19/2^-$ alternative for the isomer.

In addition to the yrast band, which is highlighted in Fig. 11, more unfavored signature non-yrast rotational bands are predicted. Since interband transitions dominate over

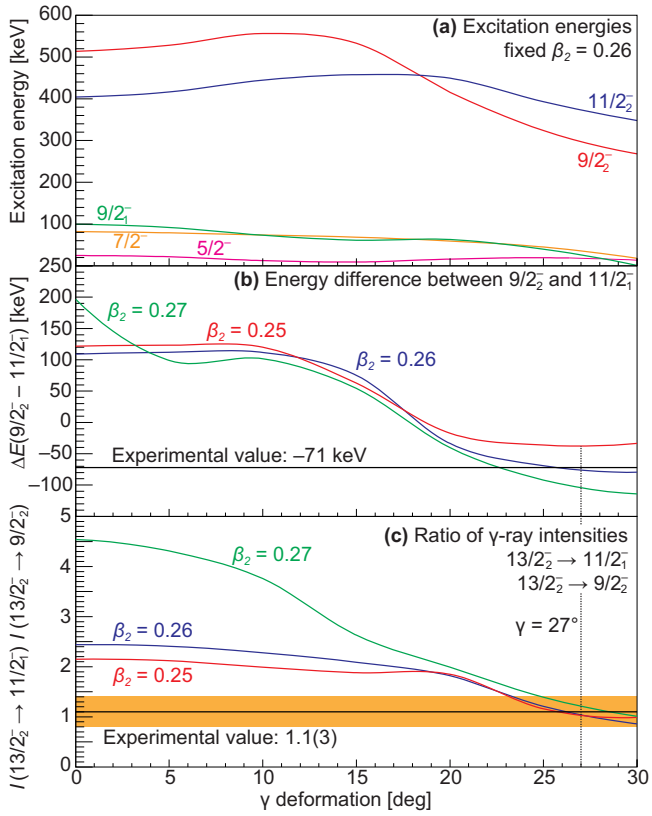

FIG. 10. (a) Excitation energies of the $5/2^-$, $7/2^-$, $9/2_1^-$, $9/2_2^-$, and $11/2_2^-$ states, relative to the $3/2^-$ state, calculated with the PTRM with fixed $\beta_2 = 0.26$ and $\beta_4 = 0.02$ deformation parameters. (b) Energy differences between the $9/2_2^-$ and $11/2_2^-$ states for three different values of β_2, calculated with the PTRM. The experimentally determined value is given. (c) Ratio of γ-ray intensities between $13/2_2^- \rightarrow 11/2_1^-$ and $13/2_2^- \rightarrow 9/2_2^-$ transitions, calculated with the PTRM. The experimentally determined value is given.

intraband transitions, it is difficult to observe complete bands by means of in-beam spectroscopy. Note that part of such a band is known in ^{183}Au [14], and possible fragments of unfavored signature bands were observed in ^{181}Au [12], but they were not interpreted.

The calculation predicts a $19/2^+$ state, located between the $17/2^+$ and $21/2^+$ yrast states; see Fig. 11. The $19/2^+$ state is indicated with red color. This state is predicted to deexcite dominantly into the $17/2^+$ yrast state via a transition with a predominantly $M1$ multipolarity. Only a weak transition into the $15/2^+$ state is predicted. Therefore, the 1041 keV state, observed in the present work, is assigned as $19/2^+$. Note that this assignment is tentative. Multipolarities of the 701.9 and 372.7 keV transitions need to be established to make an unambiguous conclusion on the spin-parity.

A $15/2^+$ state, located between the $13/2^+$ and $17/2^+$ yrast states, is predicted by the calculation. The tentative 900 keV excited state is a candidate for the predicted $15/2^+$ state.

Using the PTRM model, the $9/2^+ - 13/2^+$ and $21/2^+ - 19/2^+$ energy differences were investigated as a function of γ, with fixed β_2 and β_4 deformation parameters. Results of these calculations are given in Fig. 12. Note that the model used does not contain the variable moment of inertia approach, thus the calculated excitation energies of states in rotational bands are overestimated, compared with experiment. Therefore, the difference between the excitation energy of the known $21/2^+$ yrast state (not observed here) and the unfavoured $19/2^+$ state was investigated. The difference between the 1041 keV $19/2^+$ state and the $21/2^+$ yrast state [27] is 112 keV. The close proximity of the $19/2^+$ and $21/2^+$ states suggests $\gamma \approx 20°$; see Fig. 12. Interestingly, the $19/2^+ - 21/2^+$ energy difference depends only very weakly on the axial quadrupole deformation parameter β_2 at $\gamma \approx 20°$.

The $9/2^+$ state was observed 16 keV below the $13/2^+$ bandhead [27]. The PTRM predicts the $9/2^+$ state to be slightly above the $13/2^+$ state at $\gamma \approx 20°$ for all three β_2 values; see Fig. 12. However, the excitation energy of the $9/2^+$ state can be perturbed by mixing with another $9/2^+$ state of the weakly deformed configuration, as observed in ^{177}Au; see the discussion in [27]. In that case, a mixing repulsion might reduce the excitation energy of the $9/2^+$, and thus it may appear below the $13/2^+$ bandhead, as is observed experimentally. An important point of the model is that the $13/2^+$ and $9/2^+$ states are predicted to be located close together. Therefore, the observed decay pattern is consistent with the calculation for deformation parameters $\beta_2 = 0.26$ and $\gamma = 20°$. More excited states, associated with the positive-parity intruder configuration, need to be discovered before a more accurate picture can be settled.

V. SUMMARY AND CONCLUSIONS

Excited states in the extremely neutron-deficient isotope ^{179}Au have been populated and studied using a fusion-evaporation reaction and γ-ray spectroscopy. The new results include the discovery of a new rotational band, associated with the negative-parity $1h_{9/2} \oplus 2f_{7/2}$ proton-intruder configuration, and identification of a new isomeric state with an excitation energy of 1743(17) keV and $T_{1/2} = 2.16(8)$ μs. The decay paths of the isomer proceed through both new and previously known intruder states.

Calculations based on the PTRM model were performed to interpret the data. They suggest strong triaxial deformation of both $1h_{9/2} \oplus 2f_{7/2}$and $1i_{13/2}$ proton-intruder configurations.

Several more similar isomers might exist in ^{179}Au, but they could not be identified due to limited statistics. Such structures were not observed in heavier Au isotopes as far as current spectroscopy has revealed. The search for such isomers in heavier Au isotopes appears to be very important, since they provide a unique opportunity to study otherwise inaccessible non-yrast states. Most notably in ^{181,183}Au, where possibilities of β-decay studies are strongly limited due to the $1/2^-$ spin-parity of the ground states in the ^{181,183}Hg mother isotopes.

This work clearly documents the power of the PTRM approach and its ability to "navigate" the interpretation of experimental data. It also shows the importance of combining high-statistics in-beam studies (note the critical band was populated with an intensity of 1.3% only) with decay studies, which reveal low-spin states associated with the same configurations. Although ^{179}Au is an extremely neutron-deficient

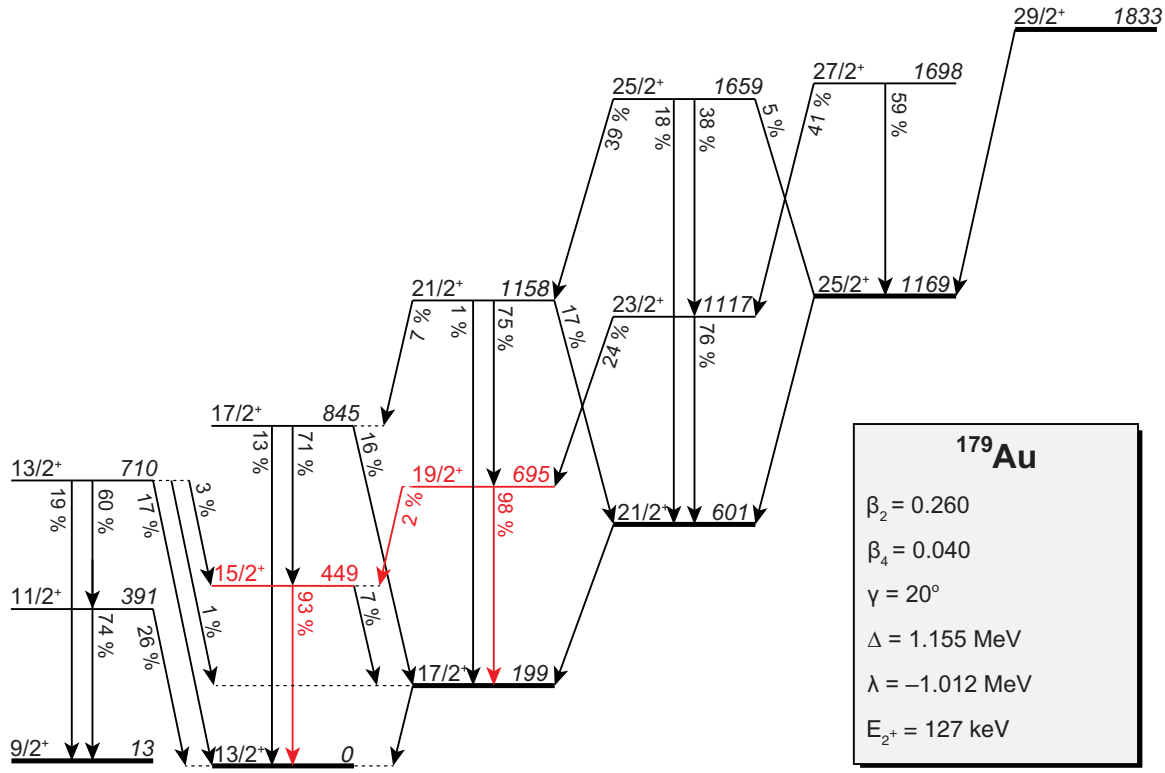

FIG. 11. Excited states associated with the $1i_{13/2}$ proton-intruder configuration calculated using the PTRM; see the text for details. Transitions between excited states are indicated together with their relative intensities. The new $15/2^+$ and $19/2^+$ states and deexciting transitions that have been experimentally observed are indicated with red color.

isotope, located 18 neutrons away from the stable Au isotope, it serves as an important point for understanding the nuclear structure of odd-mass Au isotopes.

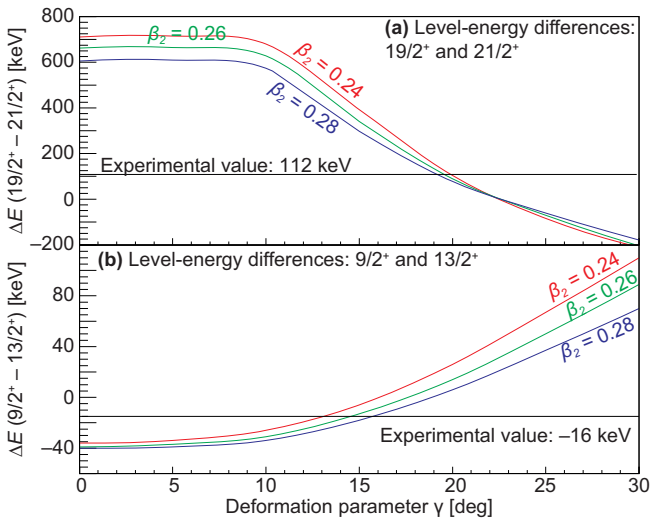

FIG. 12. Level-energy differences between (a) $9/2^+$ and $13/2^+$, (b) $21/2^+$ and $19/2^+$ states of the $1i_{13/2}$ configuration, given as a function of the triaxial deformation parameter γ for fixed $\beta_2 = 0.24$, 0.26, and 0.28. Level energies were calculated with the PTRM; see the text for details. Corresponding values, determined experimentally, are indicated by horizontal lines.

To settle the complete picture of intruder states in ^{179}Au, lifetime measurements for excited states should be performed. Such measurements would yield absolute values of reduced transition probabilities. These values provide another important constraint for the PTRM. In addition to that, the β-decay study of ^{179}Hg $\rightarrow$ ^{179}Au is highly demanding. With a foreseen 2 GeV upgrade of the ISOLDE facility, such an experiment could be performed with high statistics.

ACKNOWLEDGMENTS

The authors express their gratitude to the staff of the Accelerator Laboratory of the University of Jyväskylä for their excellent technical support. This work has been supported by the EU-FP7-IA project ENSAR (No. 262010), the Academy of Finland (CoE in Nuclear and Accelerator Based Physics, grant to T.G., Contract No. 131665), the STFC Grant No. ST/P003885/1, the European Research Council through the project SHESTRUCT (Grant Agreement No. 203481), the UK Science and Technology Facilities Council, the Slovak Research and Development Agency under Contract No. APVV-20-0532, Slovak grant agency VEGA (Contract No. 2/0067/21), and the Research and Development Operational Programme funded by the European Regional Development Fund, Project No. ITMS code 26210120023 (20%). M. Ven. acknowledges funding from the ESET Foundation (Slovakia).

[1] K. Heyde and J. L. Wood, Rev. Mod. Phys. **83**, 1467 (2011).

[2] M. Venhart, J. L. Wood, M. Sedlák, M. Balogh, M. Bírová, A. J. Boston, T. E. Cocolios, L. J. Harkness-Brennan, R.-D. Herzberg, L. Holub, D. T. Joss, D. S. Judson, J. Kliman, J. Klimo, L. Krupa, J. Lušnák, L. Makhathini, V. Matoušek, Š. Motyčák, R. D. Page *et al.*, J. Phys. G: Nucl. Part. Phys. **44**, 074003 (2017).

[3] M. Sedlák, M. Venhart, J. L. Wood, V. Matoušek, M. Balogh, A. J. Boston, T. E. Cocolios, L. J. Harkness-Brennan, R. D. Herzberg, D. T. Joss, D. S. Judson, J. Kliman, R. D. Page, A. Patel, K. Petrík, and M. Veselský, Eur. Phys. J. A **56**, 161 (2020).

[4] D. Rupnik, E. F. Zganjar, J. L. Wood, P. B. Semmes, and P. F. Mantica, Phys. Rev. C **58**, 771 (1998).

[5] M. O. Kortelahti, E. F. Zganjar, H. K. Carter, C. D. Papanicolopulos, M. A. Grimm, and J. L. Wood, J. Phys. G **14**, 1361 (1988).

[6] J. L. Wood, R. W. Fink, E. F. Zganjar, and J. Meyer-ter Vehn, Phys. Rev. C **14**, 682 (1976).

[7] E. F. Zganjar, J. L. Wood, R. W. Fink, L. L. Riedinger, C. R. Bingham, B. D. Kern, J. L. Weil, J. H. Hamilton, A. V. Ramayya, E. H. Spejewski, R. L. Mlekodaj, H. K. Carter, and W. D. Schmidt-Ott, Phys. Lett. B **58**, 159 (1975).

[8] J. L. Wood, M. O. Kortelahti, E. F. Zganjar, and P. B. Semmes, Nucl. Phys. A **600**, 283 (1996).

[9] J. K. Johansson, D. G. Popescu, D. D. Rajnauth, J. C. Waddington, M. P. Carpenter, L. H. Courtney, V. P. Janzen, A. J. Larabee, Z. M. Liu, and L. L. Riedinger, Phys. Rev. C **40**, 132 (1989).

[10] A. J. Larabee, M. P. Carpenter, L. L. Riedinger, L. H. Courtney, J. C. Waddington, V. P. Janzen, W. Nazarewicz, J. Y. Zhang, R. Bengtsson, and G. A. Lèander, Phys. Lett. B **169**, 21 (1986).

[11] P. Joshi, A. Kumar, I. M. Govil, R. P. Singh, G. Mukherjee, S. Muralithar, R. K. Bhowmik, and U. Garg, Phys. Rev. C **69**, 044304 (2004).

[12] W. F. Mueller, H. Q. Jin, J. M. Lewis, W. Reviol, L. L. Riedinger, M. P. Carpenter, C. Baktash, J. D. Garrett, N. R. Johnson, I. Y. Lee, F. K. McGowan, C. H. Yu, and S. Cwiok, Phys. Rev. C **59**, 2009 (1999).

[13] F. Soramel, P. Bednarczyk, M. Sferrazza, D. Bazzacco, D. De Acuñna, G. de Angelis, M. De Poli, E. Farnea, N. H. Medina, R. Menegazzo, L. Müller, D. R. Napoli, C. M. Petrache, C. Rossi Alvarez, F. Scarlassara, G. F. Segato, C. Signorini, J. Styczeń, and G. Vedovato, Eur. Phys. J. A **4**, 17 (1999).

[14] L. T. Song, X. H. Zhou, Y. H. Zhang, G. de Angelis, N. Marginean, A. Gadea, D. R. Napoli, M. Axiotis, C. Rusu, T. Martinez, Y. X. Guo, X. G. Lei, Y. Zheng, and M. L. Liu, Phys. Rev. C **71**, 017302 (2005).

[15] W. F. Mueller, W. Reviol, M. P. Carpenter, R. V. F. Janssens, F. G. Kondev, K. Abu Saleem, I. Ahmad, H. Amro, C. R. Bingham, J. Caggiano, C. N. Davids, D. Hartley, A. Heinz, B. Herskind, D. Jenkins, T. L. Khoo, T. Lauritsen, W. C. Ma, J. Ressler, L. L. Riedinger *et al.*, Phys. Rev. C **69**, 064315 (2004).

[16] L. T. Song, X. H. Zhou, Y. H. Zhang, Y. X. Guo, X. G. Lei, Z. Y. Sun, M. Oshima, T. Toh, A. Osa, M. Koizumi, J. Katakura, Y. Hatsukawa, M. Matsuda, and M. Sugawara, Phys. Rev. C **69**, 037302 (2004).

[17] P. Joshi, A. Kumar, G. Mukherjee, R. P. Singh, S. Muralithar, U. Garg, R. K. Bhowmik, and I. M. Govil, Phys. Rev. C **66**, 044306 (2002).

[18] F. G. Kondev, M. P. Carpenter, R. V. F. Janssens, K. Abu Saleem, I. Ahmad, H. Amro, J. A. Cizewski, M. Danchev, C. Davids, D. Hartley, A. Heinz, T. L. Khoo, T. Lauritsen, C. J. Lister, W. C. Ma, G. L. Poli, J. Ressler, W. Reviol, L. L. Riedinger, D. Seweryniak *et al.*, Phys. Lett. B **512**, 268 (2001).

[19] F. G. Kondev, M. P. Carpenter, R. V. F. Janssens, K. Abu Saleem, I. Ahmad, M. Alcorta, H. Amro, J. Caggiano, J. A. Cizewski, M. Danchev, C. N. Davids, D. J. Hartley, A. Heinz, B. Herskind, R. A. Kaye, T. L. Khoo, T. Lauritsen, C. J. Lister, W. C. Ma, G. L. Poli *et al.*, Nucl. Phys. A **682**, 487 (2001).

[20] M. Venhart, F. A. Ali, W. Ryssens, J. L. Wood, D. T. Joss, A. N. Andreyev, K. Auranen, B. Bally, M. Balogh, M. Bender, R. J. Carroll, J. L. Easton, P. T. Greenlees, T. Grahn, P.-H. Heenen, A. Herzáň, U. Jakobsson, R. Julin, S. Juutinen, D. Kĺč *et al.*, Phys. Rev. C **95**, 061302(R) (2017).

[21] H. Watkins, D. T. Joss, T. Grahn, R. D. Page, R. J. Carroll, A. Dewald, P. T. Greenlees, M. Hackstein, R. D. Herzberg, U. Jakobsson, P. M. Jones, R. Julin, S. Juutinen, S. Ketelhut, T. Kröll, R. Krücken, M. Labiche, M. Leino, N. Lumley, P. Maierbeck *et al.*, Phys. Rev. C **84**, 051302(R) (2011).

[22] T. Grahn, H. Watkins, D. T. Joss, R. D. Page, R. J. Carroll, A. Dewald, P. T. Greenlees, M. Hackstein, R.-D. Herzberg, U. Jakobsson, P. M. Jones, R. Julin, S. Juutinen, S. Ketelhut, T. Köll, R. Krücken, M. Labiche, M. Leino, N. Lumley, P. Maierbeck *et al.*, J. Phys.: Conf. Ser. **420**, 012047 (2013).

[23] T. Bäck, B. Cederwall, K. Lagergren, R. Wyss, A. Johnson, D. Karlgren, P. Greenlees, D. Jenkins, P. Jones, D. Joss, R. Julin, S. Juutinen, A. Keenan, H. Kettunen, P. Kuusiniemi, M. Leino, A.-P. Leppänen, M. Muikku, P. Nieminen, J. Pakarinen *et al.*, Eur. Phys. J. A **16**, 489 (2003).

[24] M. B. Smith, J. A. Cizewski, M. P. Carpenter, F. G. Kondev, R. V. F. Janssens, K. Abu Saleem, I. Ahmad, H. Amro, M. Danchev, C. N. Davids, D. J. Hartley, A. Heinz, T. L. Khoo, T. Lauritsen, C. J. Lister, W. C. Ma, G. L. Poli, J. J. Ressler, W. Reviol, L. L. Riedinger *et al.*, Nucl. Phys. A **682**, 433 (2001).

[25] M. Venhart, A. N. Andreyev, J. L. Wood, S. Antalic, L. Bianco, P. T. Greenlees, U. Jakobsson, P. Jones, R. Julin, S. Juutinen, S. Ketelhut, M. Leino, M. Nyman, R. D. Page, P. Peura, P. Rahkila, J. Sarén, C. Scholey, J. Sorri, J. Thomson *et al.*, Phys. Lett. B **695**, 82 (2011).

[26] G. D. Dracoulis, G. J. Lane, H. Watanabe, R. O. Hughes, N. Palalani, F. G. Kondev, M. P. Carpenter, R. V. F. Janssens, T. Lauritsen, C. J. Lister, D. Seweryniak, S. Zhu, P. Chowdhury, W. Y. Liang, Y. Shi, and F. R. Xu, Phys. Rev. C **87**, 014326 (2013).

[27] M. Venhart, M. Balogh, A. Herzáň, J. Wood, F. Ali, D. Joss, A. Andreyev, K. Auranen, R. Carroll, M. Drummond, J. Easton, P. Greenlees, T. Grahn, A. Gredley, J. Henderson, U. Jakobsson, R. Julin, S. Juutinen, J. Konki, E. Lawrie *et al.*, Phys. Lett. B **806**, 135488 (2020).

[28] J. G. Cubiss, A. E. Barzakh, A. N. Andreyev, M. Al Monthery, N. Althubiti, B. Andel, S. Antalic, D. Atanasov, K. Blaum, T. E. Cocolios, T. Day Goodacre, R. P. de Groote, A. de Roubin, G. J. Farooq-Smith, D. V. Fedorov, V. N. Fedosseev, R. Ferrer, D. A. Fink, L. P. Gaffney, L. Ghys *et al.*, Phys. Lett. B **786**, 355 (2018).

[29] K. Wallmeroth, G. Bollen, A. Dohn, P. Egelhof, U. Krönert, M. Borge, J. Campos, A. Yunta, K. Heyde, C. D. Coster, J. Wood, and H.-J. Kluge, Nucl. Phys. A **493**, 224 (1989).

[30] R. D. Harding, A. N. Andreyev, A. E. Barzakh, J. G. Cubiss, P. Van Duppen, M. Al Monthery, N. A. Althubiti, B. Andel,

S. Antalic, T. E. Cocolios, T. D. Goodacre, K. Dockx, G. J. Farooq-Smith, D. V. Fedorov, V. N. Fedosseev, D. A. Fink, L. P. Gaffney, L. Ghys, J. D. Johnson, D. T. Joss *et al.*, Phys. Rev. C **104**, 024326 (2021).

[31] U. Schrewe, P. Tidemand-Petersson, G. Gowdy, R. Kirchner, O. Klepper, A. Płochocki, W. Reisdorf, E. Roeckl, J. Wood, J. Żylicz, R. Fass, and D. Schardt, Phys. Lett. B **91**, 46 (1980).

[32] A. N. Andreyev, S. Antalic, D. Ackermann, T. E. Cocolios, V. F. Comas, J. Elseviers, S. Franchoo, S. Heinz, J. A. Heredia, F. P. Heßberger, S. Hofmann, M. Huyse, J. Khuyagbaatar, I. Kojouharov, B. Kindler, B. Lommel, R. Mann, R. D. Page, S. Rinta-Antila, P. J. Sapple *et al.*, Phys. Rev. C **80**, 024302 (2009).

[33] M. Venhart, A. N. Andreyev, J. G. Cubiss, J. L. Wood, A. E. Barzakh, C. Van Beveren, T. E. Cocolios, R. P. de Groote, D. V. Fedorov, V. N. Fedosseev, R. Ferrer, D. A. Fink, L. Ghys, M. Huyse, U. Köster, J. Lane, V. Liberati, K. M. Lynch, B. A. Marsh, P. L. Molkanov *et al.*, Phys. Rev. C **105**, 034338 (2022).

[34] C. D. Papanicolopulos, M. A. Grimm, J. L. Wood, E. F. Zganjar, M. O. Kortelahti, J. D. Cole, and H. K. Carter, Z. Phys. A: At. Nucl. **330**, 371 (1988).

[35] D. Rupnik, E. F. Zganjar, J. L. Wood, P. B. Semmes, and W. Nazarewicz, Phys. Rev. C **51**, R2867 (1995).

[36] N. Sensharma, U. Garg, Q. B. Chen, S. Frauendorf, D. P. Burdette, J. L. Cozzi, K. B. Howard, S. Zhu, M. P. Carpenter, P. Copp, F. G. Kondev, T. Lauritsen, J. Li, D. Seweryniak, J. Wu, A. D. Ayangeakaa, D. J. Hartley, R. V. F. Janssens, A. M. Forney, W. B. Walters *et al.*, Phys. Rev. Lett. **124**, 052501 (2020).

[37] S. Guo, X. Zhou, C. Petrache, E. Lawrie, S. Mthembu, Y. Fang, H. Wu, H. Wang, H. Meng, G. Li, Y. Qiang, J. Wang, M. Liu, Y. Zheng, B. Ding, W. Zhang, A. Rohilla, K. Muhki, Y. Yang, H. Ong *et al.*, Phys. Lett. B **828**, 137010 (2022).

[38] S. E. Larsson, G. A. Leander, and I. Ragnarsson, Nucl. Phys. A **307**, 189 (1978).

[39] M. Leino, J. Äystö, T. Enqvist, P. Heikkinen, A. Jokinen, M. Nurmia, A. Ostrowski, W. Trzaska, J. Uusitalo, K. Eskola, P. Armbruster, and V. Ninov, Nucl. Instrum. Methods Phys. Res., Sect. B **99**, 653 (1995).

[40] R. D. Page, A. N. Andreyev, D. E. Appelbe, P. A. Butler, S. J. Freeman, P. T. Greenlees, R.-D. Herzberg, D. G. Jenkins, G. D. Jones, P. Jones, D. T. Joss, R. Julin, H. Kettunen, M. Leino, P. Rahkila, P. H. Regan, J. Simpson, J. Uusitalo, S. M. Vincent, and R. Wadsworth, Nucl. Instrum. Methods Phys. Res., Sect. B **204**, 634 (2003).

[41] P. Rahkila, Nucl. Instrum. Methods Phys. Res., Sect. A **595**, 637 (2008).

[42] C. Baglin, Nucl. Data Sheets **110**, 265 (2009).

[43] E. S. Paul, P. J. Woods, T. Davinson, R. D. Page, P. J. Sellin, C. W. Beausang, R. M. Clark, R. A. Cunningham, S. A. Forbes, D. B. Fossan, A. Gizon, J. Gizon, K. Hauschild, I. M. Hibbert, A. N. James, D. R. LaFosse, I. Lazarus, H. Schnare, J. Simpson, R. Wadsworth, and M. P. Waring, Phys. Rev. C **51**, 78 (1995).

[44] C. Scholey, D. M. Cullen, E. S. Paul, A. J. Boston, P. A. Butler, T. Enqvist, C. Fox, H. C. Scraggs, S. L. Shepherd, O. Stezowski, A. M. Bruce, P. M. Walker, M. Caamaño, J. Garcés Narro, M. A. Bentley, D. T. Joss, O. Dorvaux, P. T. Greenlees, K. Helariutta, P. M. Jones *et al.*, Phys. Rev. C **63**, 034321 (2001).

[45] D. M. Cullen, N. Amzal, A. J. Boston, P. A. Butler, A. Keenan, E. S. Paul, H. C. Scraggs, A. M. Bruce, C. M. Parry, J. F. C. Cocks, K. Helariutta, P. M. Jones, R. Julin, S. Juutinen, H. Kankaanpää, H. Kettunen, P. Kuusiniemi, M. Leino, M. Muikku, and A. Savelius, Phys. Rev. C **58**, 846 (1998).

[46] F. Kondev, M. Carpenter, R. Janssens, C. Lister, K. Abu Saleem, I. Ahmad, H. Amro, J. Caggiano, C. Davids, A. Heinz, B. Herskind, T. Khoo, T. Lauritsen, W. Ma, J. Ressler, W. Reviol, L. Riedinger, D. Sarantites, D. Seweryniak, and I. Wiedenhoever, Phys. Lett. B **528**, 221 (2002).

[47] A. Wapstra, in *Alpha-, Beta- and Gamma-Ray Spectroscopy*, edited by K. Siegbahn (North-Holland, Amsterdam, 1965), Vol. 1, p. 539.

[48] K. H. Schmidt, Eur. Phys. J. A **8**, 141 (2000).

[49] P. Davidson, G. Dracoulis, T. Kibédi, A. Byrne, S. Anderssen, A. Baxter, B. Fabricius, G. Lane, and A. Stuchbery, Nucl. Phys. A **657**, 219 (1999).

[50] F. G. Kondev, M. P. Carpenter, R. V. F. Janssens, I. Wiedenhöver, M. Alcorta, L. T. Brown, C. N. Davids, T. L. Khoo, T. Lauritsen, C. J. Lister, D. Seweryniak, S. Siem, A. A. Sonzogni, J. Uusitalo, P. Bhattacharyya, S. M. Fischer, W. Reviol, L. L. Riedinger, and R. Nouicer, Phys. Rev. C **61**, 044323 (2000).

[51] G. D. Dracoulis, A. E. Stuchbery, A. P. Byrne, A. R. Poletti, S. J. Poletti, J. Gerl, and R. A. Bark, J. Phys. G **12**, L97 (1986).